



# A highly sensitive label-free sensor for Mercury ion ( $\text{Hg}^{2+}$ ) by inhibiting thioflavin T as DNA G-quadruplexes fluorescent inducer



Jia Ge, Xi-Ping Li, Jian-Hui Jiang, Ru-Qin Yu\*

State Key Laboratory for Chemo/biosensing and Chemometrics, College of Chemistry and Chemical Engineering, Hunan University, Changsha 410082, PR China

## ARTICLE INFO

### Article history:

Received 6 November 2013

Received in revised form

21 January 2014

Accepted 23 January 2014

Available online 31 January 2014

### Keywords:

DNA G-quadruplex

Thioflavin T

Fluorescence inducer

Label-free

Mercury ion

## ABSTRACT

DNA sequences with guanine repeats can be induced to form G-quartets that adopt G-quadruplex structures in the presence of thioflavin T (ThT). ThT plays a dual role of inducing DNA sequences to fold into quadruplex structures and of sensing the change by its remarkable fluorescence enhancement. ThT binding to the DNA sequences with guanine repeats showed highly specific fluorescence enhancement compared with single/double-stranded DNA. In this work, we have utilized the conformational switch from G-quadruplex complex induced by fluorogenic dye ThT to  $\text{Hg}^{2+}$  mediated T–Hg–T double-stranded DNA formation, thereby pioneering a facile approach to detect  $\text{Hg}^{2+}$  with fluorescence spectrometry. Through this approach,  $\text{Hg}^{2+}$  in aqueous solutions can be detected at 5 nM with fluorescence spectrometry in a facile way, with high selectivity against other metal ions. These results indicate the introduced label-free method for fluorescence spectrometric  $\text{Hg}^{2+}$  detection is simple, quantitative, sensitive, and highly selective.

© 2014 Elsevier B.V. All rights reserved.

## 1. Introduction

G-quadruplexes are a class of non-canonical four-stranded helical structures formed from guanine-rich DNA and RNA sequences, usually consisted of stacks of two or more square planar arrays of four Hoogsteen hydrogen-bonded guanines, where each base is both a hydrogen bond donor and hydrogen bond acceptor [1–3]. G-rich sequences with the potential for quadruplex formation are common in genomic DNA and these have been identified in several biologically important regions such as telomeric DNA and in many gene promoter regions [4–8]. Considering that the biological functions of G-quadruplexes may well depend on their structures, regulating the structural polymorphism of the G-quadruplexes can lead to the development of a novel methodology that can be used to investigate biological phenomena, functional molecules, and nanomaterials related to G-quadruplexes [9–12].

G-rich sequences usually are known to fold into quadruplex structures of different topology in the presence of small molecules, or certain cationic dyes [13,14]. Recently there have been various researches of metal ions stabilizing or switching the structures of G-quadruplexes. Caused by the bioactivity or genotoxicity, the most effective ions inducing G-quadruplex formation include  $\text{K}^+$ ,

$\text{Na}^+$  and  $\text{Pb}^{2+}$  ions [15–21]. Typically, compared with  $\text{K}^+$  ions which induce a mixed population of both parallel and antiparallel structures,  $\text{Na}^+$  ions only cause antiparallel quadruplex folding in 22AG human telomeric DNA (AGGGTTAGGGTTAGGGTTAGGG) [18]. Among various G-quadruplexes being investigated, the DNA oligonucleotide PS2.M is of particular interest, because it shows enhanced peroxidase activity when complexed with hemin [22]. PS2.M also has been reported to fold into a G-quadruplex in the presence of  $\text{K}^+$  ions [23–25].

In comparison with  $\text{K}^+$  ions,  $\text{Pb}^{2+}$  ions have a higher efficiency for stabilizing G-quadruplexes, due to the formation of more compact DNA folds. A previous study demonstrated that  $\text{Pb}^{2+}$ -stabilized G-quadruplexes generally have shorter M–O and O–O bonds than those stabilized by  $\text{K}^+$  ions [17]. Such compact structures contribute to the unusually high efficiency of  $\text{Pb}^{2+}$  ions in stabilizing G-quadruplexes [17,20]. Liu et al. [26] demonstrated that  $\text{Pb}^{2+}$  ions induce structural transition of the G-quadruplex of PS2.M that have been stabilized by  $\text{Na}^+$  or  $\text{K}^+$  ions, which may be ascribed to the exchange of  $\text{Pb}^{2+}$  with  $\text{Na}^+$  or  $\text{K}^+$  ions and the generation of a more compact structure.

To date, induce a conformational change of G-quadruplex by  $\text{Hg}^{2+}$  has not been reported. Interestingly, a fluorogenic dye ThT can induce G-rich oligonucleotide sequences to fold into quadruplexes and to sense the quadruplexes motif through fluorescence light-up in a visible region [27]. Highly specific fluorescence enhancement has been shown in quadruplex structures compared with the single/double-stranded DNA forms. We find the G-rich

\* Corresponding author. Tel./fax: +86 73188821916.

E-mail address: [rqyu@hnu.edu.cn](mailto:rqyu@hnu.edu.cn) (R.-Q. Yu).

sequences containing many T loop residues which can fold into quadruplex structures with ThT as inducer can also be destroyed by  $\text{Hg}^{2+}$ . It could be ascribed to the  $\text{Hg}^{2+}$  has a specific and strong binding to T residues, which leads to G-quadruplexes formation changed to double-strand DNA forms via  $\text{Hg}^{2+}$ -mediated formation of T–T base pairs. In this case, the formation of G-quadruplex structures is no longer allowed. With this thought in mind, here we investigate the inhibitory effect of  $\text{Hg}^{2+}$  on the DNA G-quadruplex via  $\text{Hg}^{2+}$ -mediated formation of T–T base pairs, aiming to develop a novel method for aqueous  $\text{Hg}^{2+}$  detection.

The oligonucleotide probe1 (GGGTTTTGGGTTTTGGGTTTTGGG) with many T loop residues was selected that can fold into a G-quadruplex structure [28]. We conjecture  $\text{Hg}^{2+}$  mediated T–Hg–T double-stranded DNA formation may has better properties because of higher structural stability. So  $\text{Hg}^{2+}$  may able to inhibit the proper folding G-quadruplex of probe1 due to its specific and strong binding to T residues in presence of ThT. On the basis of the above rationale, in this work, we utilize probe1 to specifically detect  $\text{Hg}^{2+}$  in aqueous solutions by measuring the ThT fluorescence intensity which is related with the changes of the G-quadruplex structure when  $\text{Hg}^{2+}$  inhibits ThT binding. The experimental observations confirm the method can be used for label free  $\text{Hg}^{2+}$  quantitative determination in aqueous solutions with high selectivity and sensitivity.

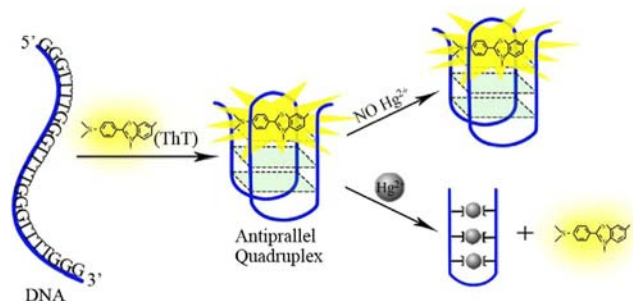
## 2. Experimental

### 2.1. Materials

Purified oligonucleotides were obtained from Sangon Biotechnology Co., Ltd. (Shanghai, China). ThT (3, 6-dimethyl-2-(4-dimethylaminophenyl) benzo-thiazolium cation) was purchased from Sigma-Aldrich Chemical Corporation. The used metal salts ( $\text{Hg}(\text{Ac})_2$ ,  $\text{Pb}(\text{Ac})_2$ ,  $\text{Mg}(\text{Ac})_2$ ,  $\text{Ca}(\text{Ac})_2$ ,  $\text{AgNO}_3$ ,  $\text{Co}(\text{NO}_3)_2$ ,  $\text{Ni}(\text{NO}_3)_2$ ,  $\text{Mn}(\text{Ac})_2$ ,  $\text{Zn}(\text{Ac})_2$ , and  $\text{Cu}(\text{Ac})_2$ ) were purchased from Sinopharm Group Chemical Reagent Co., Ltd. (Shanghai, China). All reagents were used as received without further purification. All solutions were prepared using ultrapure water, which was obtained through a Millipore Milli-Q water purification system (Billerica, MA, USA) and had an electric resistance  $> 18.3 \text{ M}\Omega$ . Before use, absorption spectra was recorded with a Shimadzu model 2450 UV–vis spectrophotometer, and the ThT concentration was calculated using the molar extinction coefficient at 412 nm in water of  $36,000 \text{ M}^{-1} \text{ cm}^{-1}$  [29]. The stock solution of ThT (10 mM) was prepared in ultrapure water, stored in the dark at  $-20^\circ\text{C}$ , and diluted to the required concentration with aqueous buffer.

### 2.2. Fluorescence measurement of $\text{Hg}^{2+}$

All measurements were performed in 10 mM Tris–HCl buffer (pH 7.6) under air at ambient temperature ( $25^\circ\text{C}$ ), unless specified



**Scheme 1.** Scheme for the  $\text{Hg}^{2+}$  inhibit ThT folding G-rich DNA with many T loop residues into the G-quadruplex.

otherwise. Briefly,  $20 \mu\text{L}$  of  $2.5 \mu\text{M}$  oligonucleotide probe was added to  $160 \mu\text{L}$  of  $7.5 \mu\text{M}$  ThT solution and then was incubated for 30 min. Then, the typical  $\text{Hg}^{2+}$  assay was performed for 30 min after adding a given concentration  $\text{Hg}^{2+}$ . Steady-state fluorescence spectra were recorded using a Hitachi F-7000 spectrofluorimeter (Hitachi, Japan) in a wavelength ranging from 450 to 530 nm. For steady-state fluorescence measurements, the samples were excited at 425 nm. Fluorescence intensity at 490 nm was used for quantitative analysis of  $\text{Hg}^{2+}$ .

## 3. Results and discussion

### 3.1. Design and construction of the biosensor for $\text{Hg}^{2+}$ detection

ThT is a fluorogenic dye with weak fluorescent by itself, but exhibits a dramatic fluorescence enhancement upon binding to DNA molecular G-quadruplexes formation. However, similar properties were not observed in the presence of duplex, triplex or single-stranded nucleic acid structures. This allows us to utilize ThT as a fluorescent reporter to induce the formation of the G-quadruplex structure and monitor its conformational change.

As  $\text{Hg}^{2+}$  is able to specifically bind to T residues of DNA, here we utilize the T-containing oligonucleotides probe1 with excellent changes in its structure to sense  $\text{Hg}^{2+}$  in aqueous solutions. Scheme 1 depicts the design and procedure of this sensor for  $\text{Hg}^{2+}$  detection. Induced by ThT and in the absence of  $\text{Hg}^{2+}$ , probe1 is able to fold into a G-quadruplex, which strongly binds ThT to form the ThT–G-quadruplex, giving rise to high fluorescence enhancement. However, with the addition of  $\text{Hg}^{2+}$ , the G-quadruplex structure of probe1 is inhibited by the  $\text{Hg}^{2+}$ -mediated formation of T–T base pairs and thus it is not able to fold into a G-quadruplex structure. As a result, the formation of ThT–G-quadruplex is no longer formed and ThT is released. This will be reflected by a fluorescence decrease when monitored by using fluorescence spectroscopy.

### 3.2. Typical characteristics of the developed biosensor for $\text{Hg}^{2+}$ detection

We hypothesized that the T–Hg–T interaction has higher efficiency than DNA molecular G-quadruplex formation, which lead to DNA not to bind with ThT due to the conformational change. To test the hypothesis, fluorescence signal change was utilized to reveal the binding of G-quadruplexes to ThT. Fig. 1A shows the fluorescence spectra (excited at  $\lambda=425 \text{ nm}$ ) of ThT in different conditions. Free ThT showed quite weak fluorescent was observed (blank curve in Fig. 1A). In the absence of ThT, P1 was in the random coil state. Upon addition of ThT, P1 was able to fold into a bimolecular G-quadruplex, which strongly binds ThT to form the ThT–G-quadruplex. Meanwhile, the solution fluorescence had strong enhancement (red curve in Fig. 1A). Then with the addition of nano-mole level of  $\text{Hg}^{2+}$ , the fluorescence sharply decreased (blue curve in Fig. 1A) due to the fact that DNA G-quadruplexes changed to duplex nucleic acid structures, which indicated ThT was released from the G-quadruplexes owing to the conformational change. Therefore, we concluded that the fluorescence decrease was caused only by  $\text{Hg}^{2+}$ .

To confirm the specificity of probe1, we tested control DNA samples the sequence probe2 (AGG GAG GGC GCT GGG AGG AGG G) and probe3 (CGA ACC CCC CCC CCC CCG AA). Probe2 is a G-rich sequence with only one T residue. From Fig. 1B we observed ThT induced probe2 to form stabilized quadruplex structure, but only slightly changed ( $< 5\%$ ) in the fluorescence intensity after adding  $\text{Hg}^{2+}$ . It was mainly because probe2 had no chance to form T–Hg–T bonds. Probe3 is a cytosine-rich single-stranded

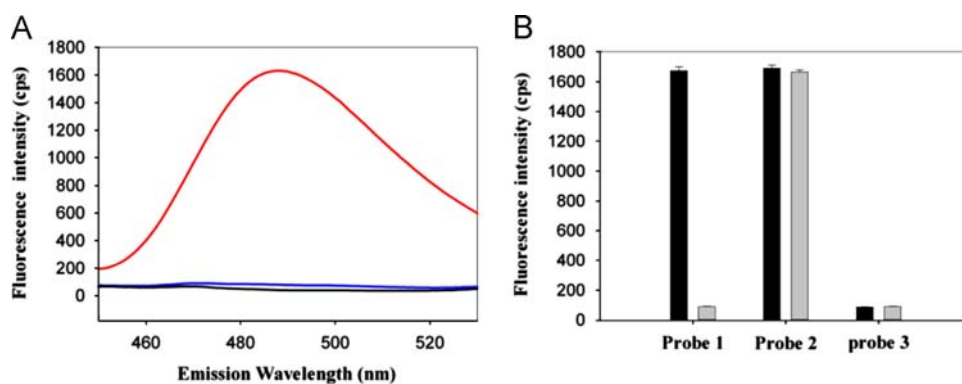


**Fig. 1.** (A) Fluorescence spectra of 10 mM Tris–HCl (pH 7.6) containing 6  $\mu\text{M}$  ThT (blank curve), 6  $\mu\text{M}$  ThT+0.25  $\mu\text{M}$  probe1 (red curve), 6  $\mu\text{M}$  ThT+0.25  $\mu\text{M}$  probe1+20  $\mu\text{M}$   $\text{Hg}^{2+}$  (blue curve). The fluorescence spectra were taken after incubating the mixture for 30 min. (B) Fluorescence intensity of probe 1 (250 nM), probe 2 (250 nM) and probe 3 (250 nM), both in mixtures of 10 mM Tris–HCl (pH 7.6) containing 6  $\mu\text{M}$  ThT, in the absence (blank histogram) and presence of 20  $\mu\text{M}$   $\text{Hg}^{2+}$  ions (gray histogram). The error bars represented for standard deviation (SD) across three repetitive experiments. (For interpretation of the references to color in this figure legend, the reader is referred to the web version of this article.)

oligonucleotide without T residue. We also observed ThT could not be able to induce the DNA probe3 to form G-Quadruplex and the fluorescence intensity changed only slightly in the presence of DNA sequences (Fig. 1B). All the measurements were performed three times. The results indicated that our present assay exhibits excellent selectivity over  $\text{Hg}^{2+}$ .

### 3.3. CD measurements

To validate the conjecture, we examined the structural changes in the DNA strand due to the addition of ThT or  $\text{Hg}^{2+}$ , using CD measurements. P1 in buffer solution (10 mM Tris, pH 7.6) displayed a characteristic CD band at 254 nm confirming its unfolded state in the absence of ThT (blue curve in Fig. 2). However, the CD spectrum showed signatures of an antiparallel quadruplex with the initial additions of ThT (red curve in Fig. 2). Then, the CD spectrum showed that the antiparallel quadruplex destroyed with the addition of  $\text{Hg}^{2+}$  (blank curve in Fig. 2).

### 3.4. Optimization of sensing conditions

Fluorescence titration experiments were then performed to obtain the maximal fluorescence signal of ThT–G-quadruplex complexes. All the measurements were performed three times. The fluorescence signal was enhanced markedly as ThT concentration was increased, and little change was observed when the concentration exceeded 6  $\mu\text{M}$  (Fig. 3A). We also found that the fluorescence signal was not affected obviously by  $\text{K}^+$  ions concentration. Even when  $\text{K}^+$  concentration was higher than 20 mM, the signal was slightly changed (Fig. 3B). Therefore, 6  $\mu\text{M}$  of ThT was used to ensure a good signal-to-background ratio and we chose Tris–HCl buffer solution without  $\text{K}^+$  ions as reaction condition to conduct experiments.

To investigate the influence of reaction temperature on ThT–G quadruplex complexes, we studied the reaction system fluorescence response in different temperature conditions (see Fig. 4A). All the measurements were performed three times. The results showed the fluorescence signal was maximum at 25  $^{\circ}\text{C}$ . A further study was performed to investigate the pH dependence of fluorescence response of ThT–G-quadruplex complexes (as shown in Fig. 4B). The fluorescence response showed only slight influence from pH 6.6 and to pH 8.4. Accordingly, a buffer solution of pH 7.6 was selected in subsequent experiments.

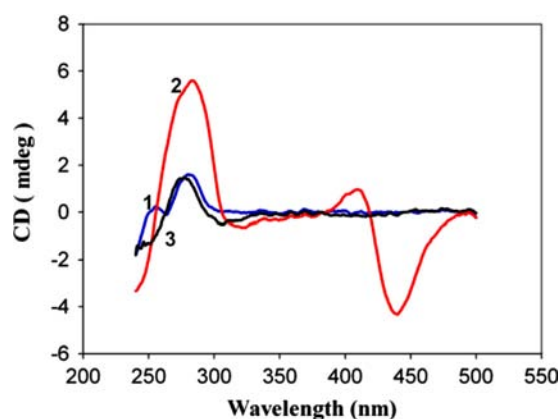


**Fig. 2.** CD spectra monitoring the conformational transition of 10  $\mu\text{M}$  probe1 (GGGTTTGGGTTTGGGTTTGGG) in Tris buffer (pH 7.6) for three modes: 1: 10  $\mu\text{M}$  probe1 (blue curve); 2: 10  $\mu\text{M}$  probe1+6  $\mu\text{M}$  ThT (red curve); 3: 10  $\mu\text{M}$  probe1+6  $\mu\text{M}$  ThT+100  $\mu\text{M}$   $\text{Hg}^{2+}$  ion (blank curve). (For interpretation of the references to color in this figure legend, the reader is referred to the web version of this article.)

### 3.5. Sensitivity of assay

To demonstrate the feasibility of our proposed approach, fluorescence signals for different concentrations of  $\text{Hg}^{2+}$  were measured under the optimal conditions (10 mM Tris–HCl buffer pH 7.6, 0.25  $\mu\text{M}$  probe1). All the measurements were performed three times. Fig. 5 illustrated increasing concentrations of  $\text{Hg}^{2+}$  in the range from 0 to 20  $\mu\text{M}$  resulted in gradual decrease of fluorescence of the ThT–G-quadruplex, which was attributed to  $\text{Hg}^{2+}$  mediated T–Hg–T double-stranded DNA formation and ThT liberation. Also, the decreased fluorescence intensity was related to  $\text{Hg}^{2+}$  concentration (Fig. 5A). From Fig. 5B there is a good linear correlation between the peak intensity and the  $\text{Hg}^{2+}$  concentration in the range from 0.01 to 5  $\mu\text{M}$ . The detection limit of  $\text{Hg}^{2+}$  is 5 nM in terms of the rule of three times standard deviation over the blank response. The relative standard deviations of peak fluorescence readings were 1.2%, 0.8%, 1.5% and 0.9% in three repetitive assays of 10 nM, 100 nM, 500 nM and 5  $\mu\text{M}$   $\text{Hg}^{2+}$ . Comparison of several major optical sensors for mercury detection based on the preferential binding property of thymidines was listed in Table 1, the sensitivity of our proposed is better than previously reported Au nanoparticle based colorimetric  $\text{Hg}^{2+}$  sensors [30–32] and some other sensors [33–37] based on the formation of T–Hg–T. The result also indicated that the proposed label-free biosensor had excellent detection performance

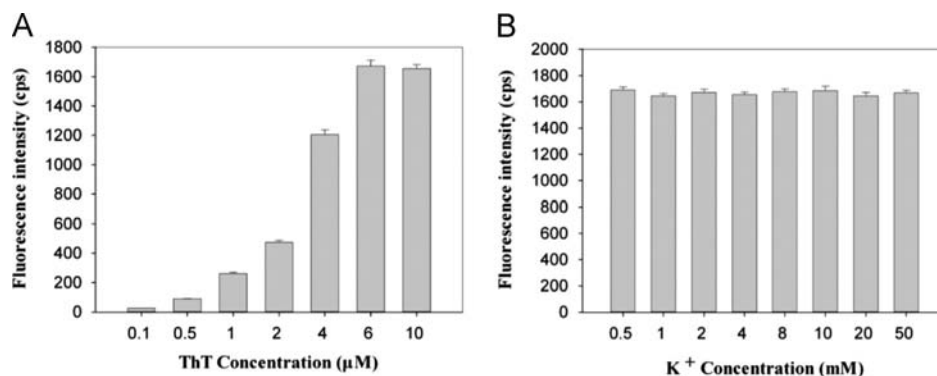


**Fig. 3.** (A) Optimization the concentration of ThT induced probe1 G-quadruplex structure formation. (B) Effection of K<sup>+</sup> ions. Experiments were carried out in a 10 mM Tris–HCl (pH 7.6) buffer containing 0.25 μM probe1 at 25 °C. The excited and emission wavelength were set at 399 nm and 490 nm, respectively. The error bars represented for standard deviation (SD) across three repetitive experiments.

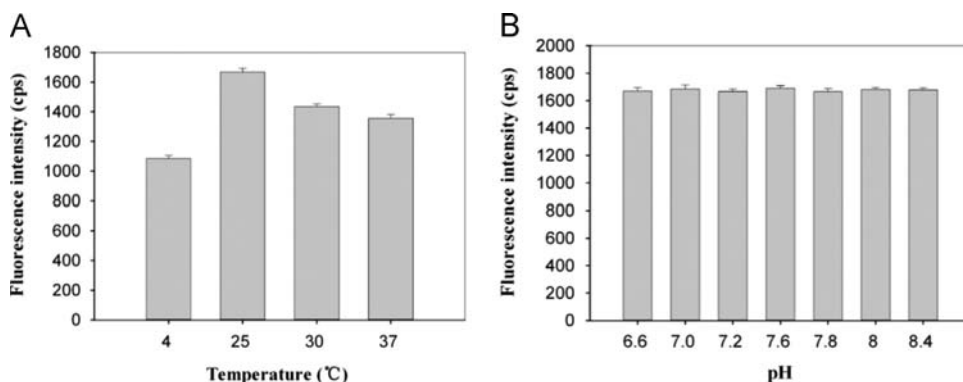


**Fig. 4.** (A) Optimization of the reaction temperature. The solution 10 mM Tris–HCl (pH 7.6) containing 6 μM ThT, 0.25 μM probe 1 at different temperature. (B) Effection of the solution pH. The solution contains 10 mM Tris–HCl (pH 6.6–pH 8.4) containing 6 μM ThT, 0.25 μM probe1 at 25 °C. The error bars represented for standard deviation (SD) across three repetitive experiments.

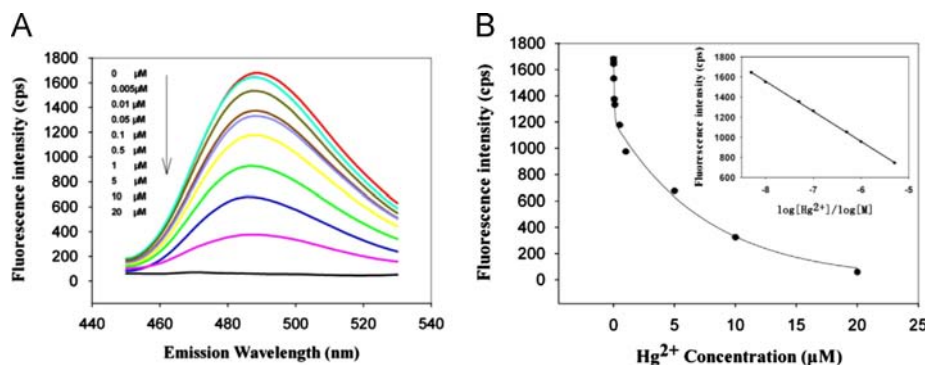


**Fig. 5.** Fluorescence spectra recorded under optimized reaction condition in the presence of (a) 0 nM, (b) 5 nM, (c) 10 nM, (d) 50 nM, (e) 100 nM, (f) 500 nM, (g) 1 μM, (h) 5 μM, (i) 10 μM, and (j) 20 μM Hg<sup>2+</sup>. The inset shows the dependence of fluorescence intensity on Hg<sup>2+</sup> concentration. The error bars represented for standard deviation (SD) across three repetitive experiments.

comparable to the previously reported of fluorescent [38–40] and chromophoric [41–43] sensors, making it suitable for drinking water monitoring.

### 3.6. Assay selectivity

To further validate the selectivity of this approach for Hg<sup>2+</sup>, competing metal ions including Mg<sup>2+</sup> and Ca<sup>2+</sup> at 100 μM, Zn<sup>2+</sup>, Co<sup>2+</sup>, Ag<sup>+</sup> and Mn<sup>2+</sup> ions at 20 μM, Pb<sup>2+</sup> and Cu<sup>2+</sup> at 5 μM, were tested under the same conditions. All the measurements were performed three times. Fig. 6 showed the effect of these cations on the fluorescence response when adding the different metal ions were added. Little change in the fluorescence intensity was

observed with addition of these metal ions. In contrast, only Hg<sup>2+</sup> caused a dramatically large fluorescence emission ratio. The results demonstrated the excellent selectivity of this approach applied in Hg<sup>2+</sup> detection.

### 3.7. Assay of Hg<sup>2+</sup> concentrations in water samples

To demonstrate the practicability of the proposed strategy in assays, we investigated the performance of the biosensor in detection of Hg<sup>2+</sup> in Mercury standard samples (IERM, Beijing, China). The analytical results are shown in Table 2. All the measurements were performed three times. We observed that the results obtained in standard samples show good recovery



**Table 1**  
Comparison of optical sensors for mercury detection.

Hg (II) ions sensor	Detection limit	Method	Reference
Au nanoparticles	100 nM	Colorimetric	[30]
Au nanoparticles	3 $\mu$ M	Naked eye	[31]
Au nanoparticles	5 $\mu$ M	Colorimetric	[32]
MSO-PMNT	42 nM	Fluorometric	[33]
MSO oligonucleotide	40 nM	Fluorometric	[34]
MSO-ThT	5 nM	Fluorometric	This work

MSO: mercury-specific oligonucleotide.

PMNT: poly (3-(3'-N,N,N-triethylamino-1'-propyloxy)-4-methyl-2,5-thiophene hydrochloride).

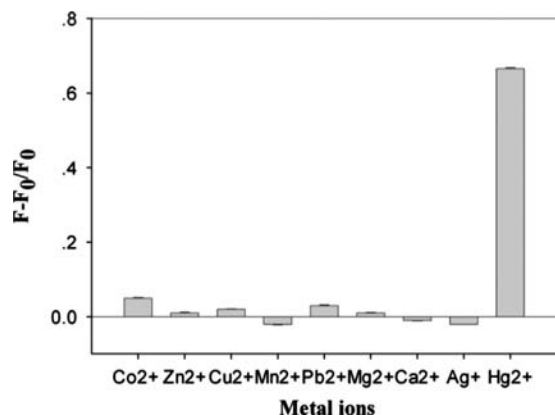


**Fig. 6.** Selectivity of ThT induced probe 1 from G-quadruplex structure to detection of Hg<sup>2+</sup>. The concentrations of Hg<sup>2+</sup> is 5  $\mu$ M and other metal ions are (Mg<sup>2+</sup> and Ca<sup>2+</sup> at 100  $\mu$ M, Zn<sup>2+</sup>, Co<sup>2+</sup>, Ag<sup>+</sup> and Mn<sup>2+</sup> ions at 20  $\mu$ M, Pb<sup>2+</sup> and Cu<sup>2+</sup> at 5  $\mu$ M) respectively. F<sub>0</sub> and F are the fluorescence intensity in the absence and presence of Hg<sup>2+</sup> respectively. The error bars represented for standard deviation (SD) across three repetitive experiments.

**Table 2**

The concentration of Hg<sup>2+</sup> in standard samples detected using the proposed biosensor.

Sample	Atomic absorption spectroscopy ( $\mu$ g L <sup>-1</sup> )	Proposed method mean <sup>a</sup> $\pm$ SD <sup>b</sup> ( $\mu$ g L <sup>-1</sup> )	Recovery (%)
Standard sample 1	5.02	4.9 $\pm$ 0.34	97.6
Standard sample 2	13.4	12.8 $\pm$ 0.23	95.5

<sup>a</sup> The mean of three determinations.

<sup>b</sup> SD=standard deviation.

values compare with the traditional method (Atomic Absorption Spectroscopy). These results, thus, exhibited that the developed biosensor was applicable for practical Hg<sup>2+</sup> detection.

The proposed method was evaluated for detection of Hg<sup>2+</sup> in river water samples obtained from Xiang River and local tap water. The river water samples collected were first filtered through a 0.22  $\mu$ m filter membrane to remove insoluble substance. The water samples were spiked with Hg<sup>2+</sup> at different concentration levels. No Hg<sup>2+</sup> was found in these samples. All the measurements were performed three times. The results are summarized in Table 3, which shows that the proposed sensor was able to detect mercury in river water and tap water samples. All the measurements were performed three times. As the toxic level for Hg<sup>2+</sup> defined by the US Environmental Protection Agency (EPA) in drinkable water is below 10 nM, the proposed assay procedure is capable of testing the Hg<sup>2+</sup> level whether the water meets the environmental standard (for instance, tap water sample 1).

**Table 3**

The concentration of Hg<sup>2+</sup> in water samples detected using the proposed biosensor.

Sample	Added [Hg <sup>2+</sup> ] (nM)	Proposed method mean <sup>a</sup> $\pm$ SD <sup>b</sup> (nM)	Recovery (%)
Tap water 1	5.0	5.14 $\pm$ 0.22	102.8
Tap water 2	20.0	19.2 $\pm$ 0.46	96
River water 1	50.0	47.6 $\pm$ 0.94	95.2
River water 2	100.0	103.5 $\pm$ 0.32	103.5

<sup>a</sup> The mean of three determinations.

<sup>b</sup> SD=standard deviation.

## 4. Conclusions

In this work, we found that for G-rich DNA sequences with many T loop residues the Hg<sup>2+</sup>-stabilized T-Hg-T is more stable than ThT induced G-quadruplex system. Therefore, Hg<sup>2+</sup> can specifically induce the formation of duplex nucleic acid DNA structures from DNA G-quartets. Based on the previous fact, a highly sensitive label-free sensor for Hg<sup>2+</sup> was designed by inhibiting ThT as DNA G-quadruplexes fluorescent inducer and selective detection of Hg<sup>2+</sup> with a detection limit of 5 nM was achieved. We believe that the present reported Hg<sup>2+</sup> sensor will provide a versatile tool for the determination of Hg<sup>2+</sup> in environmental samples. This assay also provides a highly sensitive and specific sensing platform for Hg<sup>2+</sup> bioactivity analysis.

## Acknowledgments

This work was supported by NSFC (21275002, 20905022, 21025521, 21035001, and 21190041), National Key Basic Research Program (2011CB911000), NSF of Hunan Province (10JJ7002) and Scientific Research Fund of Hunan Provincial Education Department (08A065).

## References

- [1] G. Laughlan, A.I. Murchie, D.G. Norman, M.H. Moore, P.C. Moody, D.M. Lilley, B. Luisi, *Science* 265 (1994) 520–524.
- [2] A.N. Lane, J.B. Chaires, R.D. Gray, J.O. Trent, *Nucleic Acids Res.* 36 (2008) 5482–5515.
- [3] D. Sen, W. Gilbert, *Nature* 334 (1988) 364–366.
- [4] S.L. Palumbo, R.M. Memmott, D.J. Uribe, Y. Krotova-Khan, L.H. Hurley, S.W. Ebbinghaus, *Nucleic Acids Res.* 36 (2008) 1755–1769.
- [5] P.A. Rachwal, I.S. Findlow, J.M. Werner, T. Brown, K.R. Fox, *Nucleic Acids Res.* 35 (2007) 4214–4222.
- [6] J. Seenisamy, E.M. Rezler, T.J. Powell, D. Tye, V. Gokhale, C.S. Joshi, A. Siddiqui-Jain, L.H. Hurley, *J. Am. Chem. Soc.* 126 (2004) 8702–8709.
- [7] A. Siddiqui-Jain, C.L. Grand, D.J. Bearss, L.H. Hurley, *Proc. Natl. Acad. Sci. U. S. A.* 99 (2002) 11593–11598.
- [8] D. Yang, L.H. Hurley, *Nucleosides, Nucleotides Nucleic Acids* 25 (2006) 951–968.
- [9] A. Bugaut, S. Balasubramanian, *Biochemistry* 47 (2008) 689–697.
- [10] D. Gomez, R. Paterski, T. Lemarteleur, K. Shin-ya, J.L. Mergny, J.F. Riou, *J. Biol. Chem.* 279 (2004) 41487–41494.
- [11] J.L. Huppert, S. Balasubramanian, *Nucleic Acids Res.* 33 (2007) 2908–2916.
- [12] J.E. Reed, A.A. Arnal, S. Neidle, R. Vilar, *J. Am. Chem. Soc.* 128 (2006) 5992–5993.
- [13] A.C. Bhasikuttan, J. Mohanty, H. Pal, *Angew. Chem. Int. Ed.* 46 (2007) 9305–9307.
- [14] V. Dhamodharan, S. Harikrishna, C. Jagadeeswaran, K. Halder, P.I. Pradeepkumar, *J. Org. Chem.* 77 (2012) 229–242.
- [15] F.M. Chen, *Biochemistry* 31 (1992) 3769–3776.
- [16] J.X. Dai, C. Punichihewa, A. Ambrus, D. Chen, R.A. Jones, D.Z. Yang, *Nucleic Acids Res.* 35 (2007) 2440–2450.
- [17] F.W. Kotch, J.C. Fettingter, J.T. Davis, *Org. Lett.* 2 (2000) 3277–3280.
- [18] K.W. Lim, S. Amrane, S. Bouaziz, W. Xu, Y. Mu, D.J. Patel, K.N. Luu, A.T. Phan, *J. Am. Chem. Soc.* 131 (2009) 4301–4309.
- [19] D. Sen, W. Gilbert, *Nature* 344 (1990) 410–414.
- [20] I. Smirnov, R.H. Shafer, *J. Mol. Biol.* 296 (2000) 1–5.

- [21] J.D. Zhang, J.X. Dai, E. Veliath, R.A. Jones, D.Z. Yang, *Nucleic Acids Res.* 38 (2010) 1009–1021.
- [22] P. Travascio, A.J. Bennet, D.Y. Wang, D. Sen, *Chem. Biol.* 6 (1999) 779–787.
- [23] H.W. Lee, D.J.F. Chinnapen, D. Sen, *Pure Appl. Chem.* 76 (2004) 1537–1545.
- [24] P.R. Majhi, R.H. Shafer, *Biopolymers* 82 (2006) 558–569.
- [25] P. Travascio, D. Sen, A.J. Bennet, *Can. J. Chem.* 84 (2006) 613–619.
- [26] W. Liu, H. Zhu, B. Zheng, S. Cheng, Y. Fu, W. Li, T.C. Lau, H. Liang, *Nucleic Acids Res.* 40 (2012) 4229–4236.
- [27] J. Mohanty, N. Barooah, V. Dhamodharan, S. Hari Krishna, P.I. Pradeepkumar, A.C. Bhasikuttan, *J. Am. Chem. Soc.* 135 (2013) 367–376.
- [28] D. Hu, F. Pu, Z. Huang, J. Ren, X. Qu, *Chemistry* 16 (2010) 2605–2610.
- [29] M. Groenning, L. Olsen, M. van de Weert, J.M. Flink, S. Frokjaer, F.S. Jørgensen, *J. Struct. Biol.* 158 (2007) 358–369.
- [30] C.W. Liu, Y.T. Hsieh, C.C. Huang, Z.H. Lin, H.T. Chang, *Chem. Commun.* 21 (2008) 2242–2244.
- [31] Y. Tanaka, S. Oda, H. Yamaguchi, Y. Kondo, C. Kojima, A. Ono, *J. Am. Chem. Soc.* 129 (2007) 244–245.
- [32] X.W. Xu, J. Wang, K. Jiao, X.R. Yang, *Biosens. Bioelectron.* 24 (2009) 3153–3158.
- [33] D. Han, Y.R. Kim, J.W. Oh, T.H. Kim, R.K. Mahajan, J.S. Kim, H. Kim, *Analyst* 134 (2009) 1857–1862.
- [34] X. Liu, Y. Tang, L. Wang, J. Zhang, S. Song, C. Fan, S. Wang, *Adv. Mater.* 19 (2007) 1471–1474.
- [35] A. Ono, H. Togashi, *Angew. Chem. Int. Ed.* 43 (2004) 4300–4302.
- [36] Y.X. Wang, F.H. Geng, Q.L. Cheng, H.Y. Xu, M.T. Xu, *Analyst* 136 (2011) 4284–4288.
- [37] S.M. Jia, X.F. Liu, P. Li, D.M. Kong, H.X. Shen, *Biosens. Bioelectron.* 27 (2011) 148–152.
- [38] L.Q. Guo, H. Hu, R.Q. Sun, G.N. Chen, *Talanta* 79 (2009) 775–779.
- [39] C.Y. Li, X.B. Zhang, L. Qiao, Y. Zhao, C.M. He, S.Y. Huan, L.M. Lu, L.X. Jian, G.L. Shen, R.Q. Yu, *Anal. Chem.* 81 (2009) 9993–10001.
- [40] Q.J. Ma, X.B. Zhang, X.H. Zhao, Z. Jin, G.J. Mao, G.L. Shen, R.Q. Yu, *Anal. Chim. Acta* 663 (2010) 85–90.
- [41] J.S. Lee, M.S. Han, C.A. Mirkin, *Angew. Chem. Int. Ed.* 46 (2007) 4093–4096.
- [42] X.J. Xue, F. Wang, X.G. Liu, *J. Am. Chem. Soc.* 130 (2008) 3244–3245.
- [43] S.J. He, D. Li, C.F. Zhu, S.P. Song, L.H. Wang, Y.T. Long, C.H. Fan, *Chem. Commun.* 40 (2008) 4885–4887.